Polyhedron 166 (2019) 226–232

Contents lists available at ScienceDirect

Polyhedron

journal homepage: www.elsevier.com/locate/poly

Synthesis of monosubstituted dipicolinic acid hydrazide derivative and structural characterization of novel Co(III) and Cr(III) complexes

Anita Blagus Garin [a,*], Dunja Rakarić [a], Elvira Kovač Andrić [a], Martina Medvidović Kosanović [a], Tomislav Balić [a,*], Franc Perdih [b]

[a] Department of Chemistry, Josip Juraj Strossmayer University of Osijek, Cara Hadrijana 8/A, 31000 Osijek, Croatia
[b] Faculty of Chemistry and Chemical Technology, University of Ljubljana, Vecna Pot 113, SI-1000 Ljubljana, Slovenia

ARTICLE INFO

Article history:
Received 15 January 2019
Accepted 31 March 2019
Available online 6 April 2019

Keywords:
Dipicolinic derivates acid
Hydrazide
Cobalt complexes
Chrome complexes
Isostructural crystal structures

ABSTRACT

A novel monosubstituted dipicolinic acid hydrazide derivative (***H$_2$L*** = 6-{[2-(phenylcarbonyl)hydrazino]-carbonyl}pyridine-2-carboxylic acid) was prepared by the multi-step synthesis route starting from methoxy-substituted pyridine-2,6-dicarboxylic acid. Reaction of the prepared compound with Co and Cr salts in the presence of 1,6-diaminohexane resulted in formation of discrete complex compounds (***CoL*** and ***CrL***). The synthesized compounds were identified by chemical analyses and characterized by IR spectroscopy, thermal analysis and the ligand additionally by NMR spectroscopy. The crystal and molecular structure of the prepared complexes were determined by the single-crystal X-ray diffraction and electrochemical properties by cyclic voltammetry. The molecular structure of the complex compounds is found to be isostructural with rather small differences in the crystal packing arrangement. In both complexes the coordination geometry is octahedral and each metal ion is coordinated by two mutually orthogonal ligand molecules that act as *N,N,O*-tridentate ligand. In the crystal structure, the molecules are linked *via* multiple O–H···O, N–H···O and N–H···Cl hydrogen bond interactions thus forming a supramolecular *zig-zag* motif that is additionally stabilized by a series of hydrogen bond interactions that involve water molecule, diaminohexane cation, uncoordinated oxygen atom of carboxylic group and oxygen atom of carbonyl group. Electrochemical analysis of complex compounds indicated irreversible oxidation of Cr^{3+} in ***CrL*** and reduction of Co^{3+} to Co^{2+} in ***CoL***, which agrees with the proposed oxidation state of the metal in complexes.

1. Introduction

Derivatives of pyridine 2,6-dicarboxylic acid (dpa) commonly coordinate to transition metals as partly or fully deprotonated ligands in the various coordinating modes [1]. Dipicolinic acid hydrazides are interesting multidentate chelating systems, that can be used as pharmacologically active compounds because of their diverse biological activity, such as antibacterial and anti-inflammatory properties, amphophilic characteristics, low toxicity and high anti-HIV activity [2,3,4]. Another important property of dpa is increased biological activity in the form of complex compound [5]. The biological activity of compounds with uncoordinated carboxyl group often becomes more effective and preferable upon coordination to the appropriate metal ion [6]. The nature and the oxidation state of a metal ion, type and number of coordinated ligands and conformation of the metal complexes provide numerous possibilities for design of bioactive metal complexes [7]. Many biologically important transition metal complexes with dpa derivatives are known as biomimetic drugs. Zinc cation and its complexes exhibit a high insulin mimetic activity in animal models, visible as stimulation of lipogenesis, glucose transport and incorporation into lipids and thereby decrease of the high blood glucose concentrations [8]. The drug screening process for compounds with antidiabetic effects revealed that Zn dpa complexes exhibit effective insulin-mimetic activity [9], and Co dpa complexes showed physiological action similar to insulin [10]. Number of precondition must be met in order to use coordination compounds as potential substitutes for insulin, such as high stability in the presence of other biomolecules and especially in the acidic conditions, hydrophilicity and lipophilicity must be balanced to enable absorption and transport in the blood stream, neutral charge, low molecular weight, accessible coordination sphere around metal center, bio-recognition site for transmembrane transport and low toxicity [11]. The organic chromium(III)

* Corresponding authors. Fax: +385 31 399 969.
E-mail addresses: ablagarin@gmail.com (A.B. Garin), tombalic@kemija.unios.hr (T. Balić).

https://doi.org/10.1016/j.poly.2019.03.059
0277-5387/

complexes increase chromium availability in the body and can be used as a dietary supplement for the treatment of diabetes and high cholesterol. Among these complexes with dpa are promising candidates for diabetes treatment [12,13].

The hydrazide derivatives of dpa contain a large number of potential donor atoms that are capable of coordinating to the metal center in diverse arrangements. The hydrazide dpa derivatives can be mono- or bis-substituted, depending on a subtle preparation and crystallization conditions [14]. On the multi-step synthesis route from dipicolinc acid and methyl- or benzil-hydrazide, a new mono-substituted dipicolinic acid hydrazide derivative was prepared (Scheme 1). Although compound is a potential pentadentate ligand, it can be divided into two distinct parts; tridentate dicarboxylatepyridine *O,N,O* or *O,N,N*, depending on ligand conformation, and bidentate hydrazide *N,N* donor sites. Dipicolinate and derivatives usually coordinate to transition metals in *O,N,O* chelating mode through the 2,6 pyridine dicarboxylate moiety [15]. However, when oxygen atom(s) is substituted by hydrazide moiety in dpa system, the most preferable coordination mode is *O,N,N* or *N,N,N* (mono- and bis-substituted, respectively). In this coordination mode the ligand utilizes hydrazide nitrogen atom(s), pyridine nitrogen and carboxylate oxygen atom for coordination to the metal center. Although these type of ligands are excellent candidates for preparation of transition metal complexes, with interesting physical and biological properties [16], only several examples were structurally characterized and found from the Cambridge Structural Database (CSD version 5.39) [17] search (14 transition metal complexes with dpa hydrazide derivatives). There are only 2 structurally characterized Cu complex compounds with monosubstituted hydrazide derivatives [18]. In all complexes ligands act as *N,N,N*- or *O,N,N*-chelators. However, no structures were found in the CSD database with ligand ***H$_2$L*** or close analogs. In order to evaluate the coordination properties of such ligands we prepared a novel dipicolinic acid hydrazide derivate, 6-{[2-(phenylcarbonyl)hydrazino]carbonyl}pyridine-2-carboxylic acid (***H$_2$L***) (Scheme 1) and two new coordination compounds with trivalent Co and Cr ions (***CoL*** and ***CrL***). The compounds were identified by means of chemical analyses and characterized by IR and NMR spectroscopy. The thermal properties of the compounds were investigated by TG/DSC method. Molecular and crystal structures of coordination compounds (***CoL*** and ***CrL***) were determined by the single-crystal X-ray diffraction. The compounds were also characterized by cyclic and differential pulse voltammetry.

2. Experimental section

2.1. General methods

All commercially available chemicals were of reagent grade and used as purchased. 6-(methoxycarbonyl)pyridine-2-carboxylic acid was prepared by previously reported procedure [19]. IR spectra were recorded on Shimadzu FTIR 8400S spectrophotometer using the DRS 8000 attachment, in the 4000–400 cm^{-1} region. Thermogravimetric analyses were performed using simultaneous TGA-DSC analyser (Mettler-Toledo TGA/DSC 1). The samples (approx. 20 mg–30 mg) were placed in aluminum pans (100 μL) and heated in an oxygen atmosphere (200 mL min^{-1}) up to 550 °C at a rate of 10 °C min^{-1}. The data collection and analysis was performed using the program package STAR^e Software 10.0 [20]. Elemental analyses were performed on PerkinElmer 2400 Series II CHNS/O system. ^{1}H NMR spectra were recorded with Bruker Avance III 500 (at room temperature and 500.10 MHz) magnetic resonance spectrometers with DMSO-d_6 and $CDCl_3$ as solvents and TMS as an internal reference. MS spectra were recorded with an Agilent 6224 Accurate Mass TOF LC/MS instrument.

Electrochemical experiments were performed on PalmSens potentiostat/galvanostat (PalmSens BV, Utrecht, The Netherlands) driven by PSTrace 4.2 software. A conventional three-electrode cell was used with a glassy carbon as a working electrode, non-aqueous Ag/Ag^+ as a reference electrode and a platinum wire as a counter electrode. The glassy carbon working electrode was polished with polishing α-Al_2O_3 (0.05 μm, ALS, Japan) before each measurement. Cyclic voltammetry scan rate was 150 mV s^{-1}.

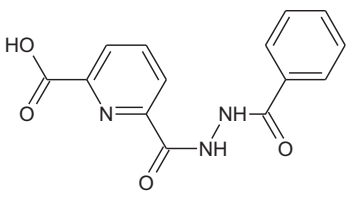

Scheme 1. Representation of ligand (***H$_2$L***).

2.2. X-ray crystallography

The single-crystal X-ray diffraction data were collected at 150 K and at room temperature on an Oxford Diffraction SuperNova CCD diffractometer with graphite-monochromated Mo Kα radiation (λ = 0.71073 Å) using ω-scans. The data reduction was performed using the CrysAlis software package [21]. The structures were solved with the SIR2004 program [22]. Refinement and analysis of the structures were done using the programs integrated within the WinGX system [23]. The refinement procedure was performed by the full-matrix least-squares method based on F^2 against all reflections using SHELXL-97 [24]. All non-hydrogen atoms were refined anisotropically. Hydrogen atoms in structures were placed in calculated positions and refined using the riding model. Geometrical calculations were done using PLATON [25,26] and the structure drawings with ORTEP and MERCURY [27] programs. The crystallographic data are summarized in Table S1.

2.3. Syntheses

2.3.1. Preparation of the ligand ***H$_2$L***

The synthesis route for preparation of ***H$_2$L*** is represented on Scheme S1. 6-(methoxycarbonyl)pyridine-2-carboxylic acid (1.61 g, 5.5 mmol) was dissolved under argon in dry dichloromethane and the mixture was stirred for 30 min at room temperature. The mixture was then cooled in an ice bath and thereafter, oxalyl chloride (1.6 ml, 18.6 mmol) and dimethylformamide (0.5 mL) were added dropwise. The mixture was stirred 30 min on ice bath and 1.5 h at room temperature. Solvent and the excess oxalyl chloride were evaporated under reduced pressure. The methyl 6-(chlorocarbonyl) pyridine-2-carboxylate (5 mmol) was dissolved in anhydride dichloromethane and stirred at room temperature. The resulting creamy mixture was cooled at 0 °C and 0.73 mL of pyridine and 1.224 g (9 mmol) of benzhydrazide were added under argon. The ice bath was removed and the red brown colored reaction mixture was stirred overnight. The solvent was removed under reduced pressure and mixture was suspended in water. The beige colored precipitate of methyl 6-{[2-(phenylcarbonyl)hydrazino]carbonyl}pyridine-2-carboxylate (2.535 g, 95%) was collected by filtration, washed with water and dried at 60 °C. IR ν_{max} (cm^{-1}): 3430; 3206; 3005; 2963; 1727; 1703; 1648; 1539; 1510; 1448; 1436; 1301; 1249; 1217; 1153; 1144; 1075; 1026; 1000; 982; 899; 847; 792; 748; 691; 675; 647; 612. **^{1}H NMR** (500 MHz, DMSO-d_6) δ 8.95 (s, 1H), 8.27 (dd, J = 7.7, 1.1 Hz, 1H), 8.21 (dd, J = 7.9, 1.1 Hz, 1H), 7.97 (t, J = 7.8 Hz, 1H), 7.82 (d, J = 7.4 Hz, 2H), 7.49 (t, J = 7.4 Hz, 1H), 7.4 (t, J = 7.6 Hz, 2H), 3,96 (s, 3H) (Fig. S7). **MS** m/z = 299.0901. *Anal.* Calc. for

$C_{15}H_{13}N_3O_4 \times 1.5\ H_2O$ (326.30): C 55.21, H 4.94, N 12.88; found: C 54.84, H 4.75, N 12.02%.

Into a methanolic solution of methyl 6-{[2-(phenylcarbonyl)hydrazino]carbonyl}pyridine-2-carboxylate (1.0 g, 3.35 mmol) 85% aqueous solution of potassium hydroxide (32 mmol) was added. Red brown colored mixture was stirred overnight. The solvent was evaporated and the mixture was then diluted with water and acidified to pH = 3 with 2 M HCl. The resulting mixture was extracted with CH_2Cl_2 (6×10 ml) and extract was dried ($MgSO_4$), filtered and evaporated. Yield of 6-{[2-(phenylcarbonyl) hydrazino]carbonyl}pyridine-2-carboxylic acid (***H₂L***) is 2.371 g (98%). IR ν_{max} (cm^{-1}): 3469; 3096; 1763; 1668; 1608; 1522; 1454; 1334; 1260; 1184; 1158; 1075; 1004; 846; 739; 685. **^{1}H NMR** (500 MHz, DMSO-d_6) δ 13.04 (s, 1H), 11.17 (d, J = 1.3 Hz, 1H), 10.70 (d, J = 1.4 Hz, 1H), 8.35–8.27 (m, 3H), 7.97–7.93 (m, 2H), 7.65–7.60 (m, 1H), 7.55 (dd, J = 8.3, 6.9 Hz, 2H) (Fig. S8). **MS** m/z = 286.0823. *Anal.* Calc. for $C_{14}H_{11}N_3O_4 \times 2.5\ H_2O$ (330.29): C 50.90, H 4.88 N 12.72; found: C 51.40, H 4.81, N 12.72%.

2.3.2. Preparation of Co and Cr complex compounds

*2.3.2.1. Preparation of $(H_3NC_6H_{12}NH_3)^{2+}[Co(L)_2]^-Cl^-\cdot H_2O$ (**CoL**).* 0.2 mmol (50 mg) of ligand ***H₂L*** were dissolved in a 4 mL of methanol with addition of a few drops of DMF and 3 M solution of NH_3. The resulting solution was heated and slowly added to a methanol solution of cobalt(II) chloride 41.6 mg (0.2 mmol). To the resulting yellow solution a methanol solution of 1,6-diaminohexane (20 mg, 0.2 mmol) was added. The resulting mixture was filtered and the filtrate was placed in a vial and left to slowly evaporate. After two weeks color of the solution changed into red and red needle like crystals suitable for diffraction experiments appeared on the edges of the vial. *Anal.* Calc. for $C_{34}H_{40}ClCoN_8O_{10}$: C, 50.1; H, 4.95; N, 13.75; Found: C, 50.34, H, 5.01; N, 14.03. IR ν_{max} (cm^{-1}): 3251(m), 1648(s), 1590(m), 1518(m), 1379(s), 750(m), 695(m), 611(w), 440(w).

*2.3.2.2. Preparation of $(H_3NC_6H_{12}NH_3)^{2+}[Cr(L)_2]^-Cl^-\cdot H_2O$ (**CrL**).* 0.2 mmol (47 mg) of chromium(III) chloride were dissolved in a 3 mL of methanol. To the resulting green solution a methanol solution of 1,6-diaminohexane 40 mg (0.4 mmol) was added. 0.2 mmol (50 mg) of ligand ***H₂L*** were dissolved in a 4 mL of methanol with addition of few drops of DMF and aqueous 3 M NH_3 solution. The metal salt and diaminohexane solution was added dropwise to the ligand solution. The resulting green colloidal solution was left to slowly evaporate. After several weeks, brown rhomboidal crystals suitable for diffraction experiments appeared at the bottom of the vial. *Anal.* Calc. for $C_{34}H_{40}ClCr\ N_8O_{10}$: C, 50.53; H, 4.99; N, 13.86; Found: C, 50.13, H, 4.68; N, 13.55%. IR ν_{max} (cm^{-1}): 3548 (m), 3396(m), 3100(s), 2038(m), 1649(s), 1570(m), 1513(m), 1346(s), 729(m), 695(m), 480(w), 453(w).

3. Results and discussion

3.1. Syntheses

The complexes were prepared by the reaction of ligand and metal chloride salts in basic conditions at room temperature and atmospheric conditions. We suppose that the presence of 1,6-diaminohexane has an important role in complex formation. It acts both as a cationic species and neutralizes overall negative charge of complex compound and most probably is involved in stabilization of higher oxidation states of metal cations. However, the most important role of diaminoexane is in a formation of crystal structures, which is discussed in details, *vide infra*. Interestingly, cobalt(II) chloride was used as a starting material, but in ***CoL*** complex cobalt is in +3 oxidation state. Most probably, the oxidation of cobalt occurred due to presence of air atmosphere and small amounts of ammonia.

3.2. Crystal structure of complexes

*3.2.1. Crystal structure of **CoL***

X-ray analysis of ***CoL*** has shown that the compound crystallizes in monoclinic crystal system, centrosymmetric space group $C\ 2/c$. The crystal structure of ***CoL*** is shown in Fig. 1 and the selected bond lengths and angles are presented in Table 1. The complex compound is comprised of one cobalt(III) atom, two ligand molecules, a non-coordinated chloride anion, diaminohexane cation and water molecule. (Fig. 1).

The cobalt ion is located on the inversion center of symmetry and octahedrally coordinated with two mutually orthogonal ligand molecules (dihedral angle between pyridine rings of 81.42(7)°). The anionic ligand act as *N*,*N*,*O*-tridentate ligand, and each of them is coordinated to the metal with two nitrogen atoms (pyridine and hydrazide) and one oxygen atom of carboxylic group, thus forming two five-membered chelate rings per ligand. The overall charge of the complex ion is negative and neutralized by the presence of hexanediamine cation and chloride anion. The coordination geometry around the cobalt atom is distorted octahedral indicated by deviations in Co-N and Co-O bond lengths and bond angles (Fig. 1, Table 1). The Co-N and Co-O bond lengths are in accordance with previously reported Co(III) complexes with hydrazide [28] and monodentate carboxylic acid derivatives [29]. In comparison to the Co(II) complexes with these functional groups the bonds are significantly shorter indicating +3 oxidation state of the cobalt ion [30].

Considering molecular features of the deprotonated ligand ***H₂L***, the bond distances and angles of donor atom groups are within normal ranges [31]. The N2–N3, C7–N2 and N3–C8 bond lengths exhibit values typical for coordination compounds with hydrazide derivatives [32]. The C–O bond lengths of carboxylic acid group (1.222(2) and 1.227(2) Å) indicate resonant form of the same group. The ligand is non-planar molecule with largest deviation

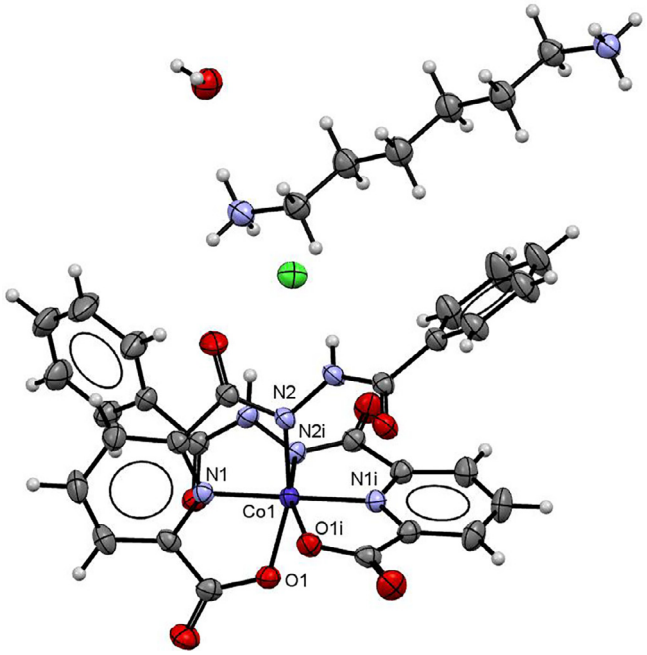

Fig. 1. ORTEP plot of ***CoL*** with displacement ellipsoids of non-hydrogen atoms drawn at 50% probability level. Only coordination sphere atoms are labeled due to clarity. (i) $-x, -y, -z$.

Table 1
Selected interatomic bond distances (Å) and bond angles (°) for ***CoL*** and ***CrL***.

CoL			
Co(1)–N(1)	1.8540(1)	N(1)–Co(1)–N(1)#1	179.80(9)
Co(1)–N(2)	1.9239(1)	N(1)–Co(1)–N(2)	81.29(6)
Co(1)–O(1)	1.9637(1)	N(1)–Co(1)–N(2)#1	98.57(6)
O(4)–C(8)	1.229(2)	N(2)–Co(1)–N(2)#1	89.68(9)
O(2)–C(6)	1.234(2)	N(1)–Co(1)–O(1)	82.36(6)
N(3)–C(8)	1.352(2)	N(2)–Co(1)–O(1)	163.64(6)
N(3)–N(2)	1.3875(1)	N(1)–Co(1)–O(1)#1	97.78(6)
O(1)–C(6)	1.288(2)	N(2)–Co(1)–O(1)#1	93.44(6)
O(3)–C(7)	1.226(2)	O(1)–Co(1)–O(1)#1	88.07(7)
N(1)–C(1)	1.334(2)		
N(1)–C(5)	1.334(2)		
C(8)–C(9)	1.492(2)		
N(4)–C(17)	1.490(2)		
N(2)–C(7)	1.351(2)		
CrL			
Cr(1)–N(1)	1.9853(1)	N(1)–Cr(1)–N(1)#2	175.99(9)
Cr(1)–O(1)	2.0122(1)	N(1)–Cr(1)–O(1)	104.25(6)
Cr(1)–N(2)	2.0331(1)	O(1)#2–Cr(1)–O(1)	89.10(8)
O(1)–C(6)	1.292(2)	N(1)–Cr(1)–N(2)#2	99.84(6)
N(1)–C(5)	1.336(2)	O(1)–Cr(1)–N(2)#2	155.91(5)
N(1)–C(1)	1.337(2)	N(1)–Cr(1)–N(2)	77.24(6)
O(4)–C(8)	1.233(2)	N(1)–Cr(1)–O(1)#2	78.68(6)
N(2)–C(7)	1.348(2)	O(1)–Cr(1)–N(2)	95.99(6)
N(2)–N(3)	1.400(2)	N(2)#2–Cr(1)–N(2)	88.94(9)
O(2)–C(6)	1.224(2)		
N(3)–C(8)	1.343(2)		
O(3)–C(7)	1.223(2)		
N(4)–C(17)	1.491(3)		

Symmetry codes: #1 $-x, y, -z+3/2$, #2 $-x+1, y, -z+1/2$.

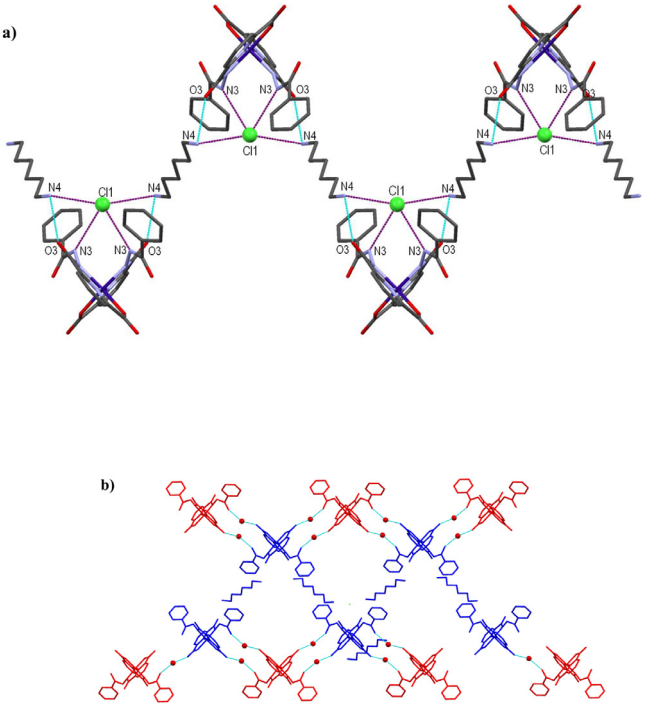

Fig. 2. (a) Representation of *zig-zag* supramolecular motif in ***CoL*** (hydrogen atoms are omitted for clarity). N–H···O and N–H···Cl interactions are represented by light blue and magenta dashed lines, respectively. (b) Representation of O–H···O hydrogen bond interactions along *b*-axis in ***CoL*** (hydrogen atoms are omitted for clarity, blue molecules represent a part of *zig-zag* supramolecular motif). O–H···O hydrogen bonds are represented by light blue dashed lines and water oxygen atoms are presented as spheres.

of phenyl ring (C9–C14) (80.99(1)°) from the plane calculated through pyridine ring.

In the crystal structure, the complex units are primarily linked *via* multiple O–H···O, N–H···O and N–H···Cl hydrogen bond interactions. Diaminohexane cations connect two discrete complex compounds *via* strong N–H···O hydrogen bond interactions, approximately along-101 crystallographic directions, thus forming supramolecular *zig-zag* motif (Fig. 2a, Table 1). The *zig-zag* structure is additionally stabilized by a series of N–H···Cl interactions that include chlorine anions, diaminohexane cations and uncoordinated hydrazide nitrogen atoms.

The resulting *zig-zag* chains are mutually connected through several hydrogen bond interactions of water molecules and uncoordinated oxygen atoms of carboxyl group (O_2 atom) along *b*-axis (Fig. 2b, Table 2). The final 3D arrangement is achieved through multiple hydrogen bond interactions that involve water molecules, diaminohexane cations, uncoordinated oxygen atoms of carboxyl group (O_2 atom) and oxygen atoms of carbonyl group (O_3) approximately along 1 −1 0 crystallographic directions.

3.2.2. Crystal structure of *CrL*

X-ray analysis of ***CrL*** has shown that the compound crystallizes in monoclinic crystal system, centrosymmetric space group *C* 2/*c*. The molecular structure of ***CrL*** is shown in Fig. 3 and the selected bond lengths and angles are presented in Table 1. The molecular structure of ***CrL*** is isostructural to ***CoL*** (***CoL*** and ***CrL*** structure overlay can be found in ESI, Fig. S1). As expected, bond lengths between coordinated ligand atoms and metal center in ***CrL*** are longer due to increase in the ionic radii of Cr(III) in comparison to Co(III). Some minor differences can be observed in bond angles of the coordination sphere (Table 1).

The Cr–N and Cr–O bond lengths are in accordance with previously reported Cr(III) complexes with hydrazide and dipicolinic acid derivatives [33].

As in ***CoL***, the building blocks of ***CrL*** are primarily linked through multiple O–H···O, N–H···O and N–H···Cl hydrogen bond interactions. Interestingly, crystal packing arrangement is almost identical as in ***CoL*** (Fig. 4, Table 3), with some minor differences in hydrogen bond geometry. Therefore it can be concluded: (*i*) that the presence of different metal cation (Cr(III)) in this type of coordination compounds has almost insignificant impact on the crystal structure, (*ii*) that packing of molecules is driven by the presence of uncoordinated species in crystal structure (diaminohecxane cation, water molecule and chlorine anion).

3.3. IR spectroscopy

3.3.1. IR spectrum of ligand (*H_2L*)

The IR spectrum of the prepared ligand (Fig. S2) is characterized by presence of strong and sharp bands at 3484 cm^{-1} and 1769 cm^{-1} that are assigned to stretching vibrations of OH group and carboxylic acid group, respectively. The C=O stretching vibration of keto group appears at 1666 cm^{-1} and the C=N stretching vibration of pyridine ring appears at 1620 cm^{-1}. The stretching vibration of the secondary amine group appears at 3170 cm^{-1} (N–H stretching vibration) and at 1500 (C–N stretching vibration). Several medium to strong vibrations assigned to the C–H bending vibration bands of *meta* and *mono* substituted benzene rings appear in 780–680 cm^{-1} region.

3.3.2. IR spectra of complexes (*CrL* and *CoL*)

In comparison to the IR spectrum of the ligand, spectra of complexes display several different bands. Both spectra are characterized by presence of broad strong band approximately at 3000 cm^{-1} that is assigned to OH stretching vibration of uncoordinated water molecules. The OH stretching vibration of carboxylic group observed in the spectrum of uncoordinated ligand is not present in spectra of complexes, indicating presence of deprotonated

Table 2
Hydrogen bond geometry (Å, °) for ***CoL***.

D–H···A	d(D–H)	d(H···A)	d(D···A)	<(DHA)	Symmetry code
N3–H3AcCl1	0.880(1)	2.464(1)	3.284(2)	155.13(1)	*x*, *y*, *z*
N4–H4A···O5	0.910(2)	1.978(2)	2.861(2)	163.04(1)	*x*, *y*, *z*
N4–H4B···O3	0.910(2)	2.215(2)	2.843(2)	125.60(1)	*x*, *y*, *z*
N4–H4C···Cl1	0.910(2)	2.317(1)	3.224(2)	174.52(1)	*x*, *y*, *z*
O5–H5B···O4	0.913(1)	1.994(1)	2.904(2)	173.91(1)	*x* − 1/2, +*y* − 1/2,+*z*
O5–H5A···O2	0.973(2)	1.864(1)	2.826(2)	169.48(1)	*x*, −*y*, +*z* − 1/2
N4–H4A···O2	0.910(2)	2.778(2)	3.228(2)	111.80(1)	−*x* − 1/2, +*y* − 1/2, −*z* + 1/2 + 1
N4–H4B···O4	0.910(2)	2.374(1)	3.033(2)	129.25(1)	−*x*, −*y*, −*z* + 1

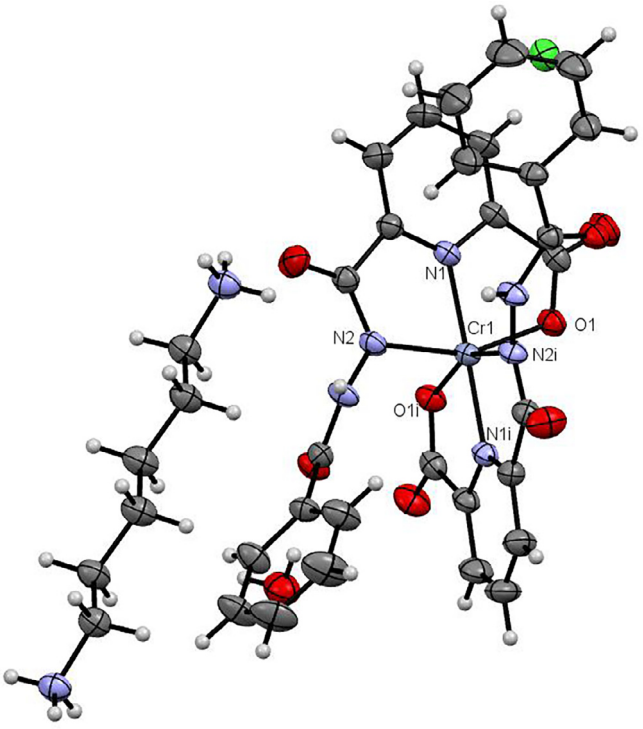

Fig. 3. ORTEP plot of ***CrL*** with displacement ellipsoids of non-hydrogen atoms drawn at 50% probability level. Only coordination sphere atoms are labeled due to clarity. (i) −*x*, −*y*, −*z*.

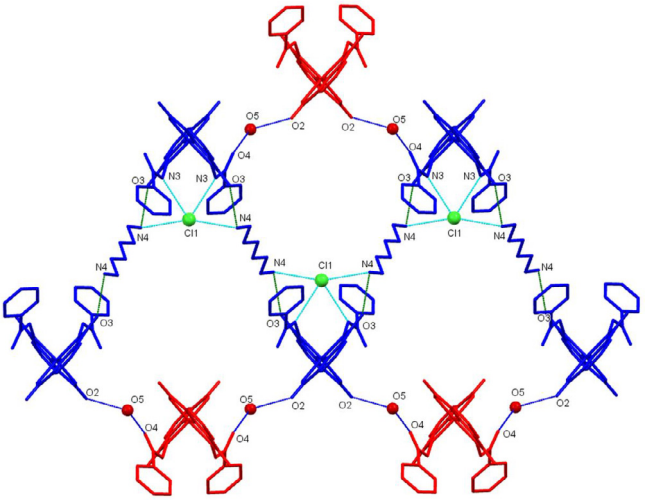

Fig. 4. Representation of packing arrangement in ***CrL*** (hydrogen atoms are omitted for clarity, chlorine ions and water oxygen atoms are presented as spheres). N–H···O and N–H···Cl interactions are represented by light green and light blue dashed lines, respectively. O–H···O hydrogen bonds are represented by blue dashed lines and water oxygen atoms are presented as spheres.

carboxylic group, and therefore coordination of ligand to metal cations. The stretching vibrations of pyridine C=N and keto C=O group in complexes are shifted to the slightly lower values in comparison to the ligand (red shift). This observation indicates that the pyridine C=N group is involved in the formation of metal–ligand bonds. The red-shift of keto C=O group can be explained by involvement of the oxygen atom in hydrogen bonding. Asymmetric and symmetric vibrations of carboxylic groups are located at 1647 cm^{-1} and 1379 cm^{-1} ($\Delta\nu$ = 268 cm^{-1}) and at 1649 cm^{-1} and 1346 cm^{-1} ($\Delta\nu$ = 303 cm^{-1}) for ***CoL*** and ***CrL***, respectively. The $\Delta\nu$ value indicates monodentate coordination of carboxylic group to the metal center [34]. The broad O–H stretching band of water molecule in ***CoL*** is superimposed to C–H and N–H stretching bands of the aliphatic chain and terminal amino group of the uncoordinated amine cation. In the spectrum of ***CrL*** there are two weak maxima located at 3458 cm^{-1} and 3396 cm^{-1} that can be assigned to N–H stretching vibrations of aliphatic diamine cation. IR spectra of complexes can be found in ESI (Figs. S3 and S4).

3.4. NMR spectroscopy of the ligand

^{1}H NMR spectra were recorded at 298 K using the residual signals δ = 7.26 ppm from $CDCl_3$ and δ = 2.50 from DMSO as an internal references. In both ^{1}H NMR spectra presence of two signals between 8.95 ppm and 11.22 ppm are assigned to protons from two NH groups. Both compounds possess two aromatic rings with eighth protons. Two doublet sets (8.21–8.27 ppm) and one triplet (7.97 ppm) are assigned to picolinato part of ligand, were signals of two triplets (7.40–7.50 ppm) and one doublet at 7.82 ppm indicate phenolic hydrogens in ***L***. Another important feature of compound methyl 6-{[2-(phenylcarbonyl)hydrazino]carbonyl}-pyridine-2-carboxylate is visible as a sharp singlet describing the three hydrogen atoms of the methoxy group at 3.95 ppm. The aromatic protons described as a doublet 8.00 ppm (d, 2H), located between the two mulitiplets 8.44–8.30 ppm (m, 3H) and 7.64 ppm (dt, 3H) are observed when methoxy group is replaced by hydroxy group in ***H_2L*** (Figs. S7 and S8).

3.5. Thermal analysis (TG/DSC)

Thermoanalytical data for the complexes (***CoL*** and ***CrL***) are presented in Figs. S5 and S6. The TG curve of ***CoL*** shows two-step thermal degradation. The first step is accompanied by a mass loss of 12.1% which can be attributed to the loss of one water molecule and one molecule of hexanediamine (calc. 11.6%) in the temperature interval of 40 °C–190 °C. The second step occurs in the temperature interval from 240 °C to 530 °C with a mass loss of 60.6 % accompanied by a strong broad exothermic peak on the DSC curve corresponding to thermal decomposition of the ligand. The residual mass (26.4%) is presumed to be cobalt(II) oxide. The TG curve of ***CrL*** exhibits thermal degradation in two steps. First step shows mass loss of 7.4%. This step can be attributed to the thermal desorption of water molecules (calc. 7.4%). The second step occurs

Table 3
Hydrogen bond geometry (Å, °) for ***CrL***.

D–H···A	d(D–H)	d(H···A)	d(D···A)	<(DHA)	Symmetry code
N4–H4A···O3	0.890(2) 0.850(2)	2.178(2) 2.070(1)	2.832(2) 2.916(2)	129.85(1)	*x*, *y*, *z*
O5–H5A···O4	0.890(2) 0.860(2)	2.353(1) 2.515(1)	3.238(2) 3.296(2)	173.09(1)	*x*, *y*, *z*
N4–H4C···Cl1	0.890(2) 0.860(2)	2.353(1) 2.515(1)	3.238(2) 3.296(2)	172.79(1)	*x*, *y*, *z*
N3–H3A···Cl1	0.890(2)	2.419(1)	3.047(2)	151.54(1)	$x + 1/2, +y - 1/2, +z$
N4–H4C···Cl1 N3–H3A···Cl1	0.890(2)	2.006(2)	2.869(3)	172.79(1)	$-x + 1/2, +y - 1/2, -z + 1/2$
N4–H4A···O4 N4–H4B···O5	0.850(2)	2.011(2)	2.854(2)	151.54(1)	$-x + 1/2, +y - 1/2, -z + 1/2$
O5–H5B···O2				127.82(1)	$-x + 1, -y, -z$
				163.17(1)	$x - 1/2, +y - 1/2, +z$
				171.41(1)	$-x + 1/2 + 1, -y + 1/2, -z$

in the temperature range of 230 °C–510 °C, accompanied by sharp exothermic peak detected on the DSC curve. This step corresponds to the thermal decomposition of the ligand and ionic species. The residual mass is assumed to be Cr(III) oxide (% of Cr 7.4). The calculated % of Cr in complex (6.9 %) is in a good agreement with one determined by thermal analysis.

3.6. Cyclic voltammetry studies

Electrochemical properties of ***CrL*** and ***CoL*** complexes in methanol were investigated by cyclic voltammetry. Previous electrochemical measurements showed that the redox peaks of different metal complexes could be assigned to different metal redox transitions [35–37]. A cyclic voltammogram of the ***CrL*** complex is shown in Fig. 5. Only one anodic peak (A1) is visible at a potential of 0.57 V

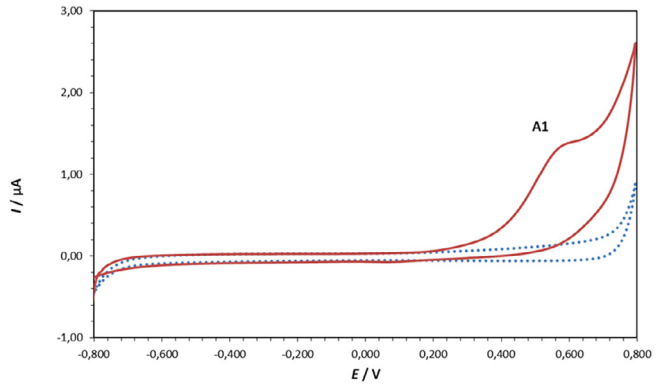

Fig. 5. Cyclic voltammogram of ***CrL*** complex ($c = 5 \times 10^{-4}$ mol dm^{-3}) at a glassy carbon electrode ($I_c = 0.1$ M LiCl in methanol). Scan rate: $\nu = 150$ mV/s. (•••) blank solution, (▬) ***CrL*** complex solution.

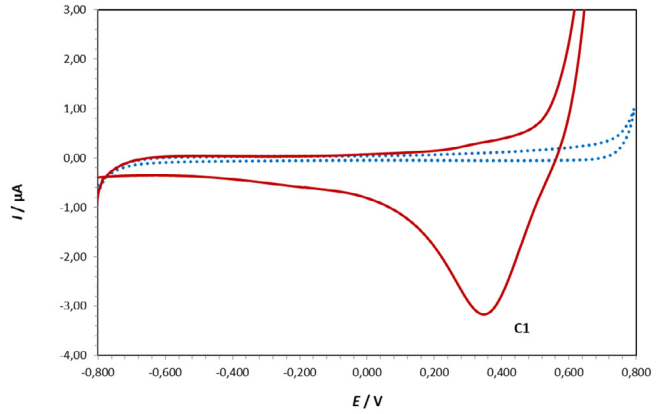

Fig. 6. Cyclic voltammogram of ***CoL*** complex ($c = 5 \times 10^{-4}$ mol dm^{-3}) at a glassy carbon electrode ($I_c = 0.1$ M LiCl in methanol). Scan rate: $\nu = 150$ mV/s. (•••) blank solution, (▬) ***CoL*** complex solution.

when it was scanned from −0.8 V to 0.8 V vs. Ag/Ag$^+$ reference electrode. This irreversible oxidation peak corresponds to oxidation of Cr^{3+} ion in the ***CrL*** complex [35].

Cyclic voltammogram of ***CoL*** complex (Fig. 6) showed one reduction peak (C1) at the potential, $E_{p,c} = 0.34$ V, which corresponds to reduction of Co^{3+} ion to Co^{2+} ion in a ***CoL*** complex (Fig. 6). This result agrees with literature data where electron transfer on a metal center in a metalloporphyrin cobalt complex was determined [35].

4. Conclusions

A novel monosubstituted dipicolinic acid hydrazide derivative (***H$_2$L*** = 6-{[2-(phenylcarbonyl)hydrazino]carbonyl}pyridine-2-carboxylic acid) was prepared and the reactions with Co and Cr salts in the presence of 1,6-diaminohexane led to the formation of discrete complex compounds (***CoL*** and ***CrL***). The single crystal structure studies of the complex compounds revealed two isostructural compounds. In the isolated complexes the coordination geometry is found to be octahedral and each metal ion is coordinated by two mutually orthogonal ligand molecules that act as *N*, *N*,*O*-tridentate ligand. Interestingly, the packing arrangement of ionic units in both complexes is almost identical, thus indicating insignificant impact of metal ion on molecular and crystal features. The dipicolinato complex anions are linked *via* series of O–H···O, N–H···O and N–H···Cl hydrogen bond interactions that involve water molecule, diaminohexane cation, uncoordinated oxygen atom of carboxyl group and oxygen atom of carbonyl group, with various forms of hydrogen bond motifs. Cyclic voltammetry revealed one oxidation peak which corresponds to Cr^{3+} oxidation in ***CrL*** complex and one reduction peak which corresponds to reduction of Co^{3+} ion to Co^{2+} in a ***CoL*** complex. The prepared compounds are among rare examples of structurally characterized mono-substituted hydrazide dpa derivatives and corresponding complexes.

Acknowledgements

This research was supported by the Ministry of Higher Education, Science and Technology of the Republic of Croatia and Slovenian Research Agency (grant no. P1-0230-0175).

Appendix A. Supplementary data

CCDC 1889940 and 1889941 contains the supplementary crystallographic data for ***CoL*** and ***CrL***. These data can be obtained free of charge via http://www.ccdc.cam.ac.uk/conts/retrieving.html, or from the Cambridge Crystallographic Data Centre, 12 Union Road, Cambridge CB2 1EZ, UK; fax: (+44) 1223-336-033; or e-mail: deposit@ccdc.cam.ac.uk. Supplementary data to this article can be found online at https://doi.org/10.1016/j.poly.2019.03.059.

References

[1] (a) M. Abdul-Kadir, L.R. Hanton, C.J. Sumby, Dalton Trans. 40 (2011) 12374;
(b) M. Napitupulu, G.A. Lawrance, G.J. Clarkson, P. Moore, Aust. J. Chem. 59 (2006) 796;
(c) A. Shatskiy, R. Lomoth, A.F. Abdel-Magied, W. Rabten, T.M. Laine, H. Chen, J. Sun, P.G. Andersson, M.D. Karkas, E.V. Johnston, B. Akermark, Dalton Trans. 45 (2016) 19024;
(d) X.-L. Wang, X. Rong, H.-Y. Lin, D.-N. Liu, X. Wang, G.-C. Liu, G. Song, Polyhedron 126 (2017) 92.
[2] J.C. Kim, A.J. Lough, H. Park, Y.C. Kang, Inorg. Chem. Commun. 9 (2006) 514.
[3] Z.A. Siddiqi, I.A. Ansari, F. Sama, M. Shahid, IJIRSET 3 (1) (2014) 8673.
[4] R.A. Al-Salahi, M.A. Al-Omar, A.E.-G.E. Amr, Molecules 15 (2010) 6588.
[5] S. Abdolmaleki, M. Ghadermazi, M. Ashengroph, A. Saffari, S.M. Sabzkohi, Inorg. Chim. Acta 480 (2018) 70.
[6] M. Devereux, M. McCann, D. O'Shea, M. O'Connor, E. Kiely, V. McKee, D. Naughton, A. Fisher, A. Kellett, M. Walsh, D. Egan, C. Deegan, Bioinorg. Chem. Appl. (2006) 80283.
[7] T.S. Kamatchi, N. Chitrapriya, H. Lee, C.F. Fronczek, F.R. Fronczek, K. Natarajan, Dalton Trans. 41 (2012) 2066.
[8] R. Jayawardena, P. Ranasinghe, P. Galappatthy, R.L.D.K. Malkanthi, G.R. Constantine, P. Katulanda, Diabetol. Metab. Syndr. 4 (2012) 13.
[9] T. Koleša-Dobravc, K. Maejima, Y. Yoshikawa, A. Meden, H. Yasui, F. Perdih, New J. Chem. 42 (2018) 3619.
[10] F. Saker, J. Ybarra, P. Leahy, R.W. Hanson, S.C. Kalhan, F. Ismail-Beigi, Am. J. Physiol. 274 (1998) E984.
[11] Z. Ma, F.E. Jacobsen, D.P. Giedroc, Chem. Rev. 109 (10) (2009) 4644.
[12] K. Ghasemi, A.R. Rezvani, I.A. Razak, A. Moghimi, F. Ghasemi, M.M. Rosli, Bull. Korean Chem. Soc. 34 (10) (2013) 3093.
[13] M.L. Lugo, V.R. Lubes, J. Chem. Eng. Data 52 (4) (2007) 1217.
[14] M. Molnar, V. Pavić, B. Šarkanj, M. Čačić, D. Vuković, J. Klenkar, Heterocycl. Commun. 23 (1) (2017) 35.
[15] (a) M. Abdul-Kadir, L.R. Hanton, C.J. Sumby, Dalton Trans. 41 (2012) 4497;
(b) M. Kla, J. Krahmer, C. Nather, F. Tuczek, Dalton Trans. 47 (2018) 1261;
(c) R. Fimognari, L.M. Cinninger, V.M. Lynch, B.J. Holliday, J. Sessler, Inorg. Chem. 57 (2017) 392.
[16] (a) V. Niel, V.A. Milway, L.N. Dawe, H. Grove, S.S. Tandon, T.S.M. Abedin, T.L. Kelly, E.C. Spencer, J.A.K. Howard, J.L. Collins, D.O. Miller, L.K. Thompson, Inorg. Chem. 47 (2008) 176;
(b) S.-N. Qin, Z.-L. Chen, D.-C. Liu, W.-Y. Huang, F.-P. Liang, Transition Met. Chem. 36 (2011) 369;
(c) N. Tyagi, O. Singh, K. Ghosh, Catal. Commun. 95 (2017) 83.
[17] C.R. Groom, I.J. Bruno, M.P. Lightfoot, S.C. Ward, Acta Crystallogr. Sect. B 72 (2016) 171.
[18] (a) Y.-M. Huang, W.-S. Wu, X.-Y. Wang, Acta Crystallogr., Sect. E 68 (2012) m783;
(b) Z.H. Li, S.X. Ma, L.Q. Kong, C. Da, Z. Li, Kristallogr. New Cryst. Struct. 229 (2014) 363.
[19] C. Schmuck, U. Machon, Chem. Eur. J. 11 (2005) 1109.
[20] STARe, Software 10.0, 2009, Mettler-Toledo GmbH.
[21] Oxford Diffraction, Oxford Diffraction Ltd., Xcalibur CCD System, CRYSALIS Software System, Version 1.171.34.44, 2010.
[22] M.C. Burla, R. Caliandro, M. Camalli, B. Carrozzini, G.L. Cascarano, L. DeCaro, C. Giacovazzo, G. Polidori, R. Spagna, J. Appl. Crystallogr. 38 (2005) 381.
[23] L.J. Farrugia, J. Appl. Crystallogr. 32 (1999) 837.
[24] G.M. Sheldrick, Acta Crystallogr., Sect. A 64 (2008) 112.
[25] A.L. Spek, Acta Crystallogr., Sect. A 46 (1990) 34.
[26] A.L. Spek, PLATON: A Multipurpose Crystallographic Tool, Ultrecht University, Ultrecht, The Netherlands, 1998.
[27] C.F. Macrae, P.R. Edgington, P. McCabe, E. Pidcock, G.P. Shields, R. Taylor, M. Towler, J. Van der Streek, J. Appl. Crystallogr. 41 (2008) 466.
[28] (a) I.O. Fritsky, R.D. Lampeka, V.V. Skopenko, Y.A. Simonov, A.A. Dvorkin, T.I. Malinowsky, Z. Naturforsch., B: Chem. Sci. 48 (1993) 270;
(b) Y.-T. Chen, J.-M. Dou, D.-C. Li, D.-Q. Wang, Y.-H. Zhu, Acta Crystallogr., Sect. E 63 (2007) m3129.
[29] (a) M. Castro, L.R. Falvello, E. Forcen-Vazquez, P. Guerra, N.A. Al-Kenany, G. Martinez, M. Tomas, Acta Crystallogr., Sect. C 73 (2017) 731;
(b) B.-H. Ye, T.-X. Zeng, P. Han, L.-N. Ji, Transition Met. Chem. 18 (1993) 515.
[30] (a) S.-N. Qin, Z.-L. Chen, D.-C. Liu, W.-Y. Huang, F.-P. Liang, Transition Met. Chem. 36 (2011) 369;
(b) M. Carcelli, S. Ianelli, P. Pelagatti, G. Pelizzi, Inorg. Chim. Acta 292 (1999) 121;
(c) T.W. Murinzi, E. Hosten, G.M. Watkins, Polyhedron 137 (2017) 188;
(d) C. Yuste, M.R. Silva, M. Ghadermazi, F. Feizi, E. Motieiyan, Acta Crystallogr., Sect. E 66 (2010) m1643.
[31] F.H. Allen, O. Kennard, D.G. Watson, L. Brammer, A.G. Orpen, R. Taylor, J. Chem. Soc., Perkin Trans. 2 (1987) 1.
[32] (a) F. Xiao, X. Dai, L. Jin, J. Coord. Chem. 61 (2008) 2402;
(b) P.V. Bernhardt, P. Chin, P.C. Sharpe, J.-Y.C. Wang, D.R. Richardson, J. Biol. Inorg. Chem. 10 (2005) 761;
(c) S.-C. Shao, S.-P. Zhang, S.-S. Chen, Z. Kristallogr. New Cryst. Struct. 226 (2011) 225;
(d) Q. Cao, D. Li, Acta Crystallogr., Sect. E 65 (2009).
[33] (a) L.S. Vojinovic-Jesic, L.S. Jovanovic, V.M. Leovac, M.M. Radanovic, M.V. Rodic, B.B. Hollo, K.M. Szecsenyi, S.A. Ivkovic, Polyhedron 101 (2015) 196;
(b) A. Moghimi, R. Alizadeh, M.C. Aragoni, V. Lippolis, H. Aghabozorg, P. Norouzi, F. Isaia, S. Sheshmani, Z. Anorg. Allg. Chem. 631 (2005) 1941;
(c) U. Casellato, R. Graziani, R.P. Bonomo, A.J. Di Bilio, J. Chem. Soc., Dalton Trans. 23 (1991) 23.
[34] G.B. Deacon, R.J. Phillips, Coord. Chem. Rev. 33 (1980) 227.
[35] M.T. de Groot, T.M. Koper, Phys. Chem. Chem. Phys. 10 (2008) 1023.
[36] D.G. Davis, D. Dolphin, Electrochemistry of Porphyrins, in the Porphyrins, Vol. 5: Physical Chemistry, Pt. C. vol. 1, Academic Press, New York, 1978, p. 137.
[37] S.O. Pinheiro, J.R. de Sousa, M.O. Santiago, I.M.M. Carvalho, A.L.R. Silva, A.A. Batista, E.E. Castellano, J. Ellena, I.S. Moreira, I.C.N. Diógenes, Inorg. Chim. Acta 359 (2006) 391–400.